

Criticality and Excitation Gap in Quantum Systems: Applications of Continuous Matrix Product States in Imaginary Time

Emanuele Tirrito,¹ Maciej Lewenstein,^{1,2} and Shi-Ju Ran^{1,*}

¹*ICFO-Institut de Ciències Fòniques, The Barcelona Institute of Science and Technology, 08860 Castelldefels (Barcelona), Spain*

²*ICREA-Institució Catalana de Recerca i Estudis Avançats, Lluís Companys 23, 08010 Barcelona, Spain*

We demonstrate an efficient method that allows for simultaneous determination of the ground state, low energy excitation properties and excitation gap in quantum many body systems. To this aim we first use the *ab-initio* optimization principle of tensor networks (TN), to show that the infinite density matrix renormalization group (iDMRG) in the real space is associated in a natural manner to the infinite time-evolving block decimation (iTEBD) implemented on a continuous matrix product state (MPS), and defined in imaginary time. We illustrate this association showing that the (imaginary) time matrix product state (MPS) in iTEBD reproduces accurately the properties of the two-dimensional (2D) classical Ising model, verifying in this way that the time MPS corresponds to a well-defined physical state. We apply then our scheme to the one-dimensional (1D) quantum Ising chain, where the time MPS is defined in continuous imaginary time. It is found that the time MPS at or close to the critical point is always maximally entangled, but gives essentially different correlations than those obtained from iDMRG; we argue that these correlations describe the dynamic correlations for the ground state.

PACS numbers: 75.40.Mg, 71.27.+a, 11.25.Hf, 02.70.-c

I. INTRODUCTION

Density matrix renormalization group (DMRG)^{1–3} and time-evolving block decimation (TEBD)^{4–7} belong to the most important algorithms in quantum many-body physics. Based on the idea of Wilson’s numeric renormalization group⁸, White proposed DMRG in 1992 to simulate the ground states of one-dimensional (1D) quantum systems^{1,2}. Its basic idea is to add one site to the block and its copy each time, then renormalize the Hilbert space by integrating out the less entangled part of basis. Beyond its original target, DMRG has been extended with great success to simulate finite-temperature thermal states^{9–11} and two-dimensional (2D) quantum models of finite size¹², as well as to simulate quantum chemistry problems¹³.

Besides the renormalization group (RG) terminology, DMRG is now better understood in the language of matrix product states (MPS) and matrix product operators (MPO)¹⁴. Specifically, the ground state obtained by DMRG was found to be an MPS that indicates a renormalization flow of the Hilbert space. Such a new perspective stimulates us to implement DMRG in a more efficient way and provides new clues for further improvements, e.g., the central matrix technique to speed up the convergence¹⁵, and a perturbation theory of DMRG to improve its accuracy¹⁶. Moreover, MPS has been proven to be extremely powerful as a variational ansatz for 1D quantum models defined on both discrete¹⁴ and continuous space^{17–19}.

Different from the RG scheme, TEBD proposed by Vidal in 2004 is a general algorithm based on tensor network (TN)^{4–7}. Using Trotter-Suzuki decomposition^{20,21}, the calculation of the ground state becomes the contraction of a 2D TN, where the TN is contracted layer by layer to an MPS until it is convergent. After each contraction, the dimension of the MPS increases, and an optimal truncation is introduced to reduce the dimension. In this sense, TEBD solves the simulation in a contraction-and-truncation (C&T) way.

The C&T scheme is very popular and useful to compute not only ground states but also general TN contraction problems. Compared with the DMRG idea, the C&T scheme is much easier to be generalized to simulate higher-dimensional systems. One famous example is tensor renormalization group (TRG)^{22–34}. In TRG, the TN is deformed by singular value decomposition (SVD) and then contracted in a certain way so that the resulting TN restores its original geometry. After each contraction, the total number of tensors in the TN decreases and the bond dimensions of the tensors increase exponentially. Then truncations, which can be obtained locally (called simple or cluster update)^{22–24,27,29,31–33} or non-locally (called full update)^{25,26,28,30,34}, are implemented to bound the dimensions. The main difference among these truncation schemes are the ways of keeping important basis by considering different environments, which lead to different accuracy and computational cost.

Recently, the *ab-initio* optimization principle (AOP) based on TN was proposed³⁵. Different from the C&T idea, AOP “encodes” an infinite TN into the summation of finite number of degrees of freedom embedded in an entanglement bath that is determined by the fixed point of a set of self-consistent equations. Interestingly, AOP explicitly shows that for infinite systems, DMRG and TEBD (dubbed as iDMRG³ and iTEBD^{6,7}, respectively) are just two eigensolvers for the same set of self-consistent eigenvalue equations. Such a unified scheme paves the way to develop new algorithms that inherit the advantages of both and to dig novel concepts to further characterize the physical systems described by the TN.

In this work, we explicitly build an equivalence between iDMRG and iTEBD based on the AOP scheme³⁵. Considering a 2D TN that can represent a 2D classical partitioning or a (1+1)-dimensional quantum theory, we show that when we do iDMRG, which is the renormalization along the spatial direction, in fact we are doing iTEBD in the other direction of the TN simultaneously, and *vice versa*. Two MPS’s are defined accordingly, which are the well-known MPS giving a real-space renormalization flow in iDMRG (dubbed as spatial

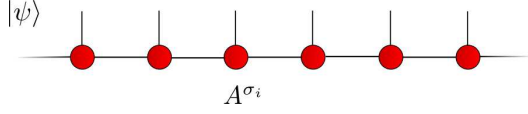


Figure 1. Graphical representation of infinite matrix product state (MPS). The tensors A^{σ_i} are in left canonical form, while the tensors B^{σ_i} are in right canonical form. λ represent the entanglement of the system.

MPS)¹⁴ and a novel translationally invariant MPS in iTEBD (dubbed as time MPS). In a 2D statistical model, we verify our scheme by showing that both MPS's give accurately the physical properties as expected. In a 1D quantum chain, we find that the time MPS defined in the continuous imaginary time exhibits different properties from the spatial MPS that corresponds to the ground state defined in the discrete space. The time MPS is a maximally entangled state and its correlation is found to be the dynamic correlation of the ground state, from which the excitation gap can be accurately obtained. Our work demonstrates that not only the ground state, but also the properties beyond (such as the excitation gap) can be accurately obtained with our TN scheme.

II. A BRIEF REVIEW OF INFINITE TIME-EVOLVING BLOCK DECIMATION AND DENSITY MATRIX RENORMALIZATION GROUP

In this section, we briefly review the formulation of iDMRG^{1,2,36} and iTEBD^{4,5}. In particular, we explain how to use these two algorithms to simulate the ground state of a 1D quantum system in the thermodynamic limit.

For the iTEBD, it follows the C&T scheme, where the ground state wave function is in an infinite MPS made of a small number of tensors that are repeated indefinitely. To obtain the optimal truncation, one transforms the MPS in its canonical form and truncate the basis according to the canonical Schmidt numbers. In this way, the truncation error is minimized.

Different from iTEBD, the real-space renormalization of the physical Hilbert space is the key in iDMRG. The ground state MPS is not explicitly translationally invariant, and actually represents a renormalization flow.

A. Infinite Matrix Product State

Here, we consider a 1D quantum chain. The physical degrees of freedom on each site give a local d -dimension Hilbert space $\mathcal{H}_d = \mathcal{C}^d$, where the local basis are denoted as $|\sigma_j\rangle$. A general form of a pure state can be written as

$$|\psi\rangle = \sum_{\sigma_1 \dots \sigma_L} C_{\sigma_1 \dots \sigma_L} |\sigma_1 \dots \sigma_L\rangle, \quad (1)$$

with $C_{\sigma_1 \dots \sigma_N}$ the coefficient matrix. One can see that the size of this matrix increases exponentially with the number

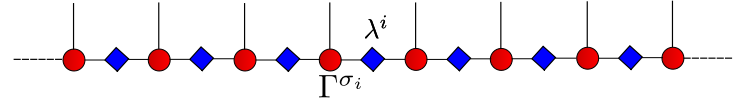


Figure 2. Graphical representation of infinite matrix product state (MPS) in canonical formulation.

of sites. To resolve such an “exponential wall”, it has been proposed to write $C_{\sigma_1 \dots \sigma_N}$ in an MPS form^{14,37,38} that reads

$$|\psi\rangle = \sum_{\{\sigma\}} \sum_{\{\beta\}} A_{1,\beta_1}^{\sigma_1} A_{\beta_1,\beta_2}^{\sigma_2} \dots A_{\beta_{L-1},1}^{\sigma_L} |\sigma_1 \dots \sigma_L\rangle, \quad (2)$$

where $A_{\beta_{i-1},\beta_i}^{\sigma_i}$ is a third-order tensor, i.e., a $(\chi_{i-1} \times \chi_i)$ matrix for each value of σ_i (χ_i the bond dimension of the virtual index β_i). Such an representation can be readily generalized to infinite systems with translationally invariant MPS, i.e. $A_{\beta\beta'}^{\sigma_i} = A_{\beta\beta'}^{\sigma_i}$ for $\forall i$. (see Fig. 1).

Given a quantum state, its MPS representation is in general not unique, but has gauge degrees of freedom. For each virtual bond β_i , we can define an invertible square matrix X_i , and rewrite the state Eq. (2) by inserting an identity in each virtual bond as

$$\dots A_{1,\beta_1}^{\sigma_1} A_{\beta_1,\beta_2}^{\sigma_2} \dots A_{\beta_{l-1},\beta_l}^{\sigma_l} \dots = \dots X_1 \left(X_1^{-1} A_{\beta_1,\beta_2}^{\sigma_2} X_2 \right) \dots \left(X_{l-1}^{-1} A_{\beta_{l-1},\beta_l}^{\sigma_l} X_l \right) \dots \quad (3)$$

The new MPS is formed by B that is again a $d \times \chi_{l-1} \times \chi_l$ tensor satisfying

$$B^{\sigma_l} = X_{l-1}^{-1} A^{\sigma_l} X_l. \quad (4)$$

The MPS Eq. (2) is then written as

$$|\psi\rangle = \sum_{\{\sigma\}} \dots B^{\sigma_1} B^{\sigma_2} \dots B^{\sigma_l} \dots |\sigma_1 \dots \sigma_l \dots\rangle, \quad (5)$$

which gives exactly the same state as that formed by A . Therefore, the gauge of MPS is equivalent to the direct sum of the groups of Isomorphisms of χ_l dimensioned complex vector spaces

$$\mathcal{G}_{MPS} = \oplus_{l=1}^{\infty} \text{Iso}(\mathcal{C}^{\chi}). \quad (6)$$

To fix the gauge, one can define the left-normalized form of the MPS, where the local tensor satisfies

$$\sum_{\sigma} A^{\sigma\dagger} A^{\sigma} = I. \quad (7)$$

Similarly, the right-normalized form is defined as

$$\sum_{\sigma} B^{\sigma} B^{\sigma\dagger} = I. \quad (8)$$

To have the translational invariance, an MPS with a positive-defined diagonal matrix on each virtual bond is introduced as (see Fig. 2)

$$|\psi\rangle = \sum_{\sigma_1 \dots \sigma_L} \Gamma^{\sigma_1} \Lambda^{[1]} \Gamma^{\sigma_2} \Lambda^{[2]} \dots \Gamma^{\sigma_{l-1}} \Lambda^{[l-1]} \Gamma^{\sigma_l} \Lambda^{[l]} \dots \Gamma^{\sigma_{L-1}} \Lambda^{[L-1]} \Gamma^{\sigma_L} |\sigma_1 \dots \sigma_L\rangle. \quad (9)$$

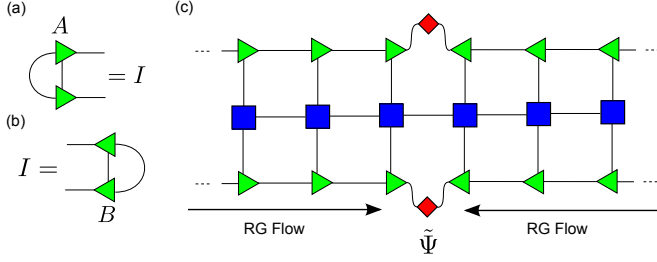


Figure 3. (Color online) The orthogonal conditions of the isometries (a) A and (b) B . (c) The MPS that appears in DMRG is formed by A , B and $\tilde{\Psi}$. Such an MPS is in the orthogonal form and gives a RG flow in the physical space of the Hamiltonian H .

In this way, the canonical form of an MPS can be defined, which is connected with the left and right orthogonal form by

$$A^{\sigma_l} = \Lambda^{[l-1]} \Gamma^{\sigma_l}, \quad B^{\sigma_l} = \Gamma^{\sigma_l} \Lambda^{[l]}. \quad (10)$$

In this form, one can prove that Γ^{σ_i} is actually the bipartite entanglement spectrum of the state.

B. Infinite density matrix renormalization group

In the DMRG scheme, one typically starts with a short block (of length l) dubbed as the system (S) and its copy as the environment (E). The basis are denoted as $\{|\alpha_l^S\rangle\}$ and $\{|\alpha_l^E\rangle\}$, respectively. Then one grows the chain to add two site between the system and the environment. Then the total state can be written as

$$|\psi\rangle = \sum_{\alpha_l^S, \sigma_{l+1}^S, \sigma_{l+1}^E, \alpha_{l+1}^E} \Psi_{\alpha_l^S \alpha_{l+1}^E}^{\sigma_A \sigma_B} |\alpha_l^S\rangle |\sigma_{l+1}^S\rangle |\sigma_{l+1}^E\rangle |\alpha_{l+1}^E\rangle, \quad (11)$$

where $|\sigma_{l+1}^S\rangle$ and $|\sigma_{l+1}^E\rangle$ represent the basis of sites added to the system and environment. The aim of the density matrix projection is to determine a subset of χ states $|\alpha_{l+1}^S\rangle$ ($|\alpha_{l+1}^E\rangle$) that optimally approximate the ground state of the enlarged system (environment) block. Accordingly, $|\alpha_{l+1}^S\rangle$ and $|\alpha_{l+1}^E\rangle$ are defined by the truncation matrices as

$$|\alpha_{l+1}^S\rangle = \sum_{\alpha_l^S} A_{\alpha_l^S \sigma_{l+1}^S, \alpha_{l+1}^S} |\alpha_l^S\rangle |\sigma_{l+1}^S\rangle, \quad (12)$$

$$|\alpha_{l+1}^E\rangle = \sum_{\alpha_l^E} B_{\alpha_l^E \sigma_{l+1}^E, \alpha_{l+1}^E} |\alpha_l^E\rangle |\sigma_{l+1}^E\rangle, \quad (13)$$

A and B are the isometries that realize the truncations of the basis, satisfying Eqs. (7) and (8) (see Fig. 11 (a) and (b)). Then the ground state with truncated basis are written as

$$|\tilde{\psi}\rangle = \sum_{\alpha_{l+1}^S \alpha_{l+1}^E} \tilde{\Psi}_{\alpha_{l+1}^S \alpha_{l+1}^E} |\alpha_{l+1}^S\rangle |\alpha_{l+1}^E\rangle. \quad (14)$$

To minimize the truncation error that is indicated by the quadratic cost function

$$S(|\tilde{\psi}\rangle) = \|\psi\rangle - |\tilde{\psi}\rangle\|^2, \quad (15)$$

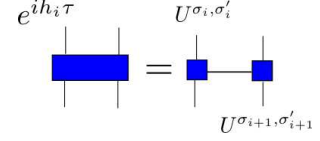


Figure 4. Graphical representation of singular value decomposition of $e^{ih_i \tau}$.

the truncation matrices is given by the dominant eigenvectors of the reduced density matrix

$$\rho_S = \text{Tr}_E |\psi\rangle \langle \psi| = \Psi \Psi^\dagger, \quad (16)$$

$$\rho_E = \text{Tr}_S |\psi\rangle \langle \psi| = \Psi^\dagger \Psi. \quad (17)$$

Then with eigenvalue decomposition, one can obtain A and B as

$$\rho_S = A D^2 A^\dagger, \quad \rho_E = B D^2 B^\dagger. \quad (18)$$

One can easily see that A , D and B in fact give the optimal singular value decomposition (SVD) of Ψ in Eq. (11), i.e.

$$\Psi_{\alpha_l^S \alpha_{l+1}^E}^{\sigma_A \sigma_B} \simeq \sum_{\alpha_{l+1}^S=1}^{\chi} A_{\alpha_l^S \sigma_{l+1}^S, \alpha_{l+1}^S} D_{\alpha_{l+1}^S} B_{\alpha_l^S \sigma_{l+1}^E, \alpha_{l+1}^E}, \quad (19)$$

showing that D gives the entanglement spectrum of the ground state.

It is well known that the ground state obtained by DMRG is actually an MPS formed by A , B and $\tilde{\Psi}$. From Fig. 3 (c), one can see that the MPS is in an orthogonal form as introduced in the last subsection, and gives a renormalization group (RG) flow of the physical Hilbert space. The direction of the RG flow is determined by the orthogonal conditions shown in Eqs. (7) and (8).

C. Infinite time-evolving block decimation

In this section we will discuss of infinite time evolving block decimation, i.e. we will show how to update the iMPS for the state $|\psi\rangle$ after an application of operator $G = e^{i\hat{H}t}$:

$$|\psi(t)\rangle = e^{i\hat{H}t} |\psi(0)\rangle, \quad (20)$$

where t can be real or imaginary. Let us assume that ψ describe an infinite translational invariant system in the form (9), and \hat{H} consists of nearest-neighbour interactions only, i.e. $\hat{H} = \sum_i \hat{h}_i$, where \hat{h}_i contains the interaction between sites i and $i+1$. We can then discretize time as $t = N\tau$ with $\tau \rightarrow 0$ and $N \rightarrow \infty$ and use the Trotter-Suzuki decomposition^{39,40}, which approximates the operator $e^{-i\hat{H}t}$. For example, the first order expansion reads:

$$e^{-i\hat{H}\tau} = e^{-i\hat{h}_1\tau} e^{-i\hat{h}_2\tau} \dots e^{-i\hat{h}_L\tau} + O(\tau^2) \quad (21)$$

which contains an error due to the non commutativity of bond Hamiltonians, $[\hat{h}_i, \hat{h}_{i+1}] = 0$. The second order expansion similarly reads:

$$e^{-i\hat{H}\tau} = e^{-\frac{i}{2}\hat{H}_{\text{odd}}\tau} e^{-i\hat{H}_{\text{even}}\tau} e^{-\frac{i}{2}\hat{H}_{\text{odd}}\tau}, \quad (22)$$

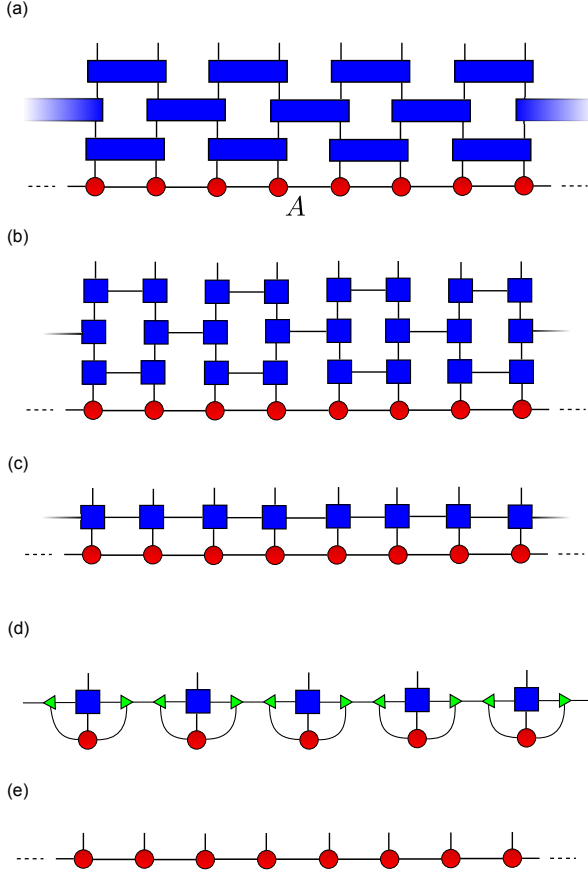


Figure 5. Graphical representation of $e^{-i\hat{H}\tau}|\psi(0)\rangle$. The operator $e^{-i\hat{H}\tau}$ is expressed in the second order Trotter decomposition.

where we have to rewrite the Hamiltonian in the following way:

$$\hat{H} = \hat{H}_{\text{odd}} + \hat{H}_{\text{even}} = \sum_{i \text{ odd}} \hat{h}_i + \sum_{i \text{ even}} \hat{h}_i. \quad (23)$$

All time evolutions on odd $e^{i\hat{H}_{\text{odd}}\tau}$ and even $e^{i\hat{H}_{\text{even}}\tau}$ bonds respectively commute among each other, and can be carried out at the same time.

So we assume $e^{-i\hat{H}\tau}$ is specified by an infinite matrix product operator iMPO^{3,15,41,42}. This iMPO is represented by a tensor $\hat{W}_{\mu,\nu}^{\sigma_i,\sigma'_i}$, where σ_i and σ'_i are physical indices and μ and ν are bond indices.

$$e^{-i\hat{H}\tau} = \hat{W}^{[1]} \hat{W}^{[2]} \dots \hat{W}^{[l]} \dots. \quad (24)$$

We can find the MPO of time evolution operator, contracting an MPO for the odd bonds and the MPO for the even bonds. Now we show how construct the MPO for the odd bonds. Let us consider the Trotter step for all odd bonds of a chain:

$$e^{-i\hat{h}_1} \otimes e^{-i\hat{h}_3} \otimes \dots e^{-i\hat{h}_{L-1}} \quad (25)$$

It would therefore be desirable to have $O^{\sigma_1,\sigma_2,\sigma'_1,\sigma'_2}$ in some form containing tensor products $O^{\sigma_1,\sigma'_1} \otimes O^{\sigma_2,\sigma'_2}$, to maintain the MPS form. At this aim we carry out a singular value

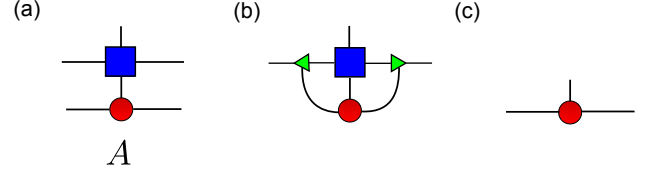


Figure 6. Graphical representation of truncation in the TEBD algorithm.

decomposition:

$$O^{\sigma_1,\sigma_2,\sigma'_1,\sigma'_2} = \sum_k U_k^{\sigma_1\sigma'_1} S_{k,k} V_k^{\sigma_2\sigma'_2\dagger} = \sum_k U_{1,k}^{\sigma_1\sigma'_1} U_{k,1}^{\sigma_2\sigma'_2}. \quad (26)$$

Moreover, the MPO representing the operator in the equation (25) is the following:

$$e^{-i\hat{H}_{\text{odd}}\tau} = U^{\sigma_1\sigma'_1} U^{\sigma_2\sigma'_2} U^{\sigma_3\sigma'_3} \dots. \quad (27)$$

Then the global MPO can be formed trivially from local MPO. Finally the algorithm occurs in two steps:

- **Contraction:** Firstly we consider the initial state in the form (9). Then we contract the tensor Γ^{σ_i} with the tensor W^{σ_i,σ'_i} of the MPO, producing an evolved iMPS characterized by the new tensor $\tilde{\Gamma}^{\sigma_i}$:

$$\tilde{A}^{\sigma_i} = \sum_{\sigma'_i} W^{\sigma_i,\sigma'_i} A^{\sigma'_i}. \quad (28)$$

The tensor λ doesn't change during the time evolution (because of the translational invariant). The bond dimension of new iMPS became $\tilde{\chi} = \chi_W \times \chi$, is larger than the rank χ of initial iMPS. The computational cost of this step is $O(d^2 \chi_W^2 \chi^2)$. Then we brought again the iMPS in canonical form.

- **Truncation:** A final iMPS is obtained from canonical form by truncating all bond indices. In particular, on each bond we preserve the first χ values of the bond indices, corresponding to the χ largest Schmidt coefficients.

III. TENSOR NETWORK ENCODING AND TIME MATRIX PRODUCT STATE

In Ref. [35], the *Ab-initio* optimization principle (AOP) for the ground states of translationally invariant many-body systems was proposed based on TN. The idea is to embed the local subsystem of a unit cell in an entanglement bath that is determined self-consistently. In the language of TN, the contraction of an infinite TN is encoded into the contraction of the original local tensor with a proper boundary. The boundary tensors are determined by a set of self-consistent eigenvalue equations.

In this section, we first briefly review the standard AOP where the matrices appearing in the eigenvalue equations are

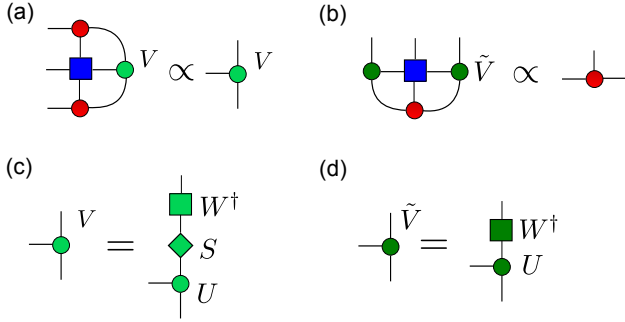


Figure 7. (Color online) The (a) and (b) show the two local eigenvalue equations given by Eqs. (31) and (32). The definition of V is shown by (c) and (d).

assumed to be Hermitian. Then by employing the idea of DMRG, we modified the eigenvalue equations to get rid of the Hermitian assumption, generalizing AOP for non-Hermitian problems. In this modified scheme, we show that two iMPS's appear along the two directions in the encoding of the 2D TN: one is the iMPS of iDMRG that represents an RG flow, and the other is the translationally invariant iMPS of iTEBD. In other words, the RG transformations in iDMRG are actually the truncations of the iMPS in iTEBD. It means that when iDMRG is implemented in one direction, in fact iTEBD is implemented at the same time in the other direction.

A. Encoding of Hermitian tensor network

The central part of AOP is to solve the self-consistent eigenvalue equations that determine the boundary tensors (denoted as A and \tilde{V}). First, one chooses a cell tensor that is defined as the only inequivalent tensor in the TN. Note there are many choices for a cell tensor, for example, a tensor properly formed by several cell tensors is still a cell tensor.

With the boundary tensors, two local eigenvalue equations are defined by two matrices (assumed to be Hermitian) as

$$M_{s_2 b_1 b'_1, s_4 b_2 b'_2} = \sum_{s_1 s_3} T_{s_1 s_2 s_3 s_4} A_{s_1 b_1 b_2}^* A_{s_3 b'_1 b'_2}, \quad (29)$$

$$\mathcal{M}_{s_1 a_1 a_2, s_3 a'_1 a'_2} = \sum_{s_2 s_4} T_{s_1 s_2 s_3 s_4} \tilde{V}_{s_2 a_1 a'_1}^* \tilde{V}_{s_4 a_2 a'_2}, \quad (30)$$

where \tilde{V} is obtained by the SVD of the boundary tensor V , i.e. $V = U S W^\dagger$, $\tilde{V} = U W^\dagger$ (Fig. 7). The tensor \tilde{V} is introduced from V in order to transform the non-local generalized eigenvalue problem to a local regular problem [Eq. (31)], where M and \mathcal{M} are required to be Hermitian. The proof can be found in the Appendix in Ref. [35]. Then, the boundary tensors A and V are obtained as the dominant eigenstates of \mathcal{M} and M , respectively, i.e.,

$$\sum_{s' a_2 a'_2} M_{s a_1 a'_1, s' a_2 a'_2} V_{s' a_2 a'_2} \propto V_{s a_1 a'_1}, \quad (31)$$

$$\sum_{s' b'_1 b'_2} \mathcal{M}_{s b_1 b_2, s' b'_1 b'_2} A_{s' b'_1 b'_2} \propto A_{s b_1 b_2}. \quad (32)$$

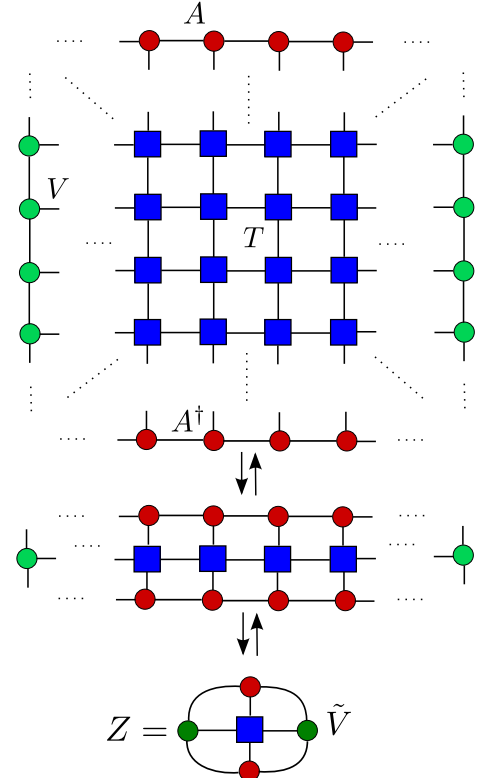


Figure 8. (Color online) In the TN encoding, one starts from an infinite TN formed by the cell tensor T with two MPS's and their conjugates defined on the boundaries along the two directions of TN. Using the eigenvalue equations (35) and (31), respectively, the TN contraction is firstly transformed into a 1D TN and then finally into a local contraction given by Eq. (33).

One can see that such two eigenvalue problems are closely related to each other: one is parametrized by the solution of the other. When the boundary tensors simultaneously solve both equations, i.e. they converge to a self-consistent fixed point, the whole infinite TN is encoded into the local contraction of the cell tensor with the boundary tensors (Fig. 8).

Specifically speaking, we start with the local contraction (a scalar) given by

$$Z = \sum T_{s_1 s_2 s_3 s_4} V_{s_2 a_1 a'_1}^* V_{s_4 a_2 a'_2} A_{s_1 a_1 a_2}^* A_{s_3 a'_1 a'_2}. \quad (33)$$

The eigenvalue equations indicate that Z is maximized by the boundary tensors. Then, we repeatedly do the substitution with Eq. (31). It should be noted that the normalization of V is required here as a constraint. Then Eq. (33) is equivalently transformed as

$$Z = \langle \psi | \rho | \psi \rangle \quad (34)$$

with $|\psi\rangle$ an infinite MPS formed by the tensor A and ρ an infinite MPO formed by T .

Then, one utilizes the fact that A is the solution of the maximization of Z . It means that the MPS $|\psi\rangle$ formed by A maximizes Eq. (34), i.e., $|\psi\rangle$ is the ground state of the MPO. In other words, we have a (non-local) eigenvalue equation

$$\rho |\psi\rangle \propto |\psi\rangle \quad (35)$$

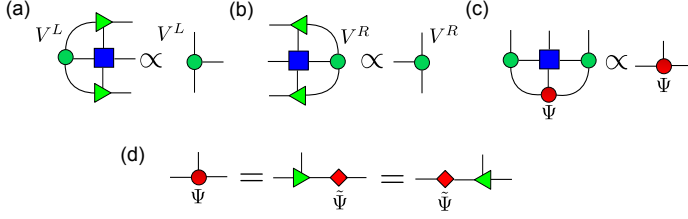


Figure 9. (Color online) The (a), (b) and (c) show the three local eigenvalue equations given by Eqs. The isometries A and B are obtained by the QR decompositions of Ψ in two different ways, as shown in (d).

under the assumption that the ground state of ρ can be effectively represented as an MPS. By substituting Eq. (35) in Eq. (34) repeatedly, the infinite TN formed by T can be reconstructed, meaning the whole TN is encoded into the local contraction given by Eq. (33). Note that for the second reconstruction with Eq. (35), the MPS $|\psi\rangle$ should be normalized. It is a non-local constraint that leads to the definition of \tilde{V} in Eq. (30).

B. A generalized tensor network encoding

In the formal subsection, the matrices in the eigenvalue equations are required to be Hermitian, so that the infinite TN contraction can be encoded into completely local problems that can be simulated in a more efficient and simple way. In this subsection, we show that iDMRG³ can be rephrased by the TN encoding scheme, where an equivalence between iDMRG and iTEBD is explicitly built.

Here, we take the one-site iDMRG as example. Comparing with the encoding of Hermitian TN, the general idea of the TN encoding given by iDMRG is the same, where the infinite TN contraction is encoded into local eigenvalue problems. But the details are quite different. As shown in Fig. 9 (a), (b) and (c), there are three local eigenvalue equations, which are given by three matrices

$$M_{s_2 b_1 b'_1, s_4 b_2 b'_2}^L = \sum_{s_1 s_3} T_{s_1 s_2 s_3 s_4} A_{s_1 b_1 b_2}^* A_{s_3 b'_1 b'_2}, \quad (36)$$

$$M_{s_2 b_1 b'_1, s_4 b_2 b'_2}^R = \sum_{s_1 s_3} T_{s_1 s_2 s_3 s_4} B_{s_1 b_1 b_2}^* B_{s_3 b'_1 b'_2}, \quad (37)$$

$$\mathcal{M}_{s_1 a_1 a_2, s_3 a'_1 a'_2} = \sum_{s_2 s_4} T_{s_1 s_2 s_3 s_4} \tilde{V}_{s_2 a_1 a'_1}^L V_{s_4 a_2 a'_2}^R. \quad (38)$$

V^L , V^R and Ψ are the eigenstate of these three matrices, respectively,

$$\sum_{s b_1 b'_1} V_{s b_1 b'_1}^L M_{s b_1 b'_1, s' b_2 b'_2}^L \propto V_{s' b_2 b'_2}^L \quad (39)$$

$$\sum_{s' b_2 b'_2} M_{s b_1 b'_1, s' b_2 b'_2}^R V_{s' b_2 b'_2}^R \propto V_{s b_1 b'_1}^R \quad (40)$$

$$\sum_{s' a'_1 a'_2} \mathcal{M}_{s a_1 a_2, s' a'_1 a'_2} \Psi_{s' a'_1 a'_2} \propto \Psi_{s a_1 a_2}. \quad (41)$$

A and B , which are the left and right orthogonal part of Ψ , are obtained by QR decomposition [Fig. 9 (d)] as

$$\Psi_{s a_1 a_2} = \sum_{a'} A_{s a_1 a'} \tilde{\Psi}_{a' a_2} = \sum_{a'} \tilde{\Psi}_{a_1 a'}^\dagger B_{s a' a_2}. \quad (42)$$

with A and B are isometries, satisfying orthogonal conditions as

$$\sum_{s a} A_{s a a_1} A_{s a a_2}^\dagger = I_{a_1 a_2}, \quad (43)$$

$$\sum_{s a} B_{s a_1 a} B_{s a_2 a}^\dagger = I_{a_1 a_2}. \quad (44)$$

The above scheme can be reinterpreted in the iDMRG language. V^L and V^R represent the system and environment super-block. \mathcal{M} is the effective Hamiltonian with Ψ its ground state. By the QR decompositions on Ψ , the renormalization of the basis of the system and environment are given by A and B , and $\tilde{\Psi}$ is the center matrix.

Similar to the AOP, the original TN can be reconstructed by repeatedly using the eigenvalue equations. We start from a local contraction (a scalar Z) of T and the boundary tensors as shown at the bottom of Fig. 10. Then with Eqs. (39) and (40), Z is transformed to the product of an MPO with an MPS and its conjugate. One can see that like iDMRG, the MPS is formed by A 's on the left side (left-orthogonal part) and B 's on the right side (right-orthogonal part) with the center matrix $\tilde{\Psi}$ in the middle. Then by using the fact that such an MPS optimally gives the ground state, we can use the corresponding eigenvalue equation to reconstruct the entire TN (Fig. 10).

In the encoding, there are three constraints: the normalizations of V^L , V^R and the MPS. The first two constraints are obviously local. For the third one, by utilizing the orthogonal conditions of A and B , the normalization of the MPS is equivalent to that of Ψ , which is also local. Thus, all eigenvalue problems are local and regular.

In the above scheme, one can explicitly see that V^L (or V^R) also gives an MPS, and interestingly, such an MPS is updated in the way of iTEBD contracting along the spatial direction. Let's pay attention to the eigenvalue equation that V^L satisfies [Eq. (39)]. If one chooses to solve it using a power method, i.e. to find the ground state of M^L by updating V^L with the product $V^L M^L$. Such a product is equivalent to evolving the local tensor of the MPS in iTEBD with the MPO formed by T in the vertical direction. In the evolution, the bond dimension of the local tensor V^L increases exponentially. Then, truncation is implemented by contracting with the isometry A .

Note that A is obtained from the QR decomposition of Ψ . Considering the eigenvalue equation [Eq. (41)], Ψ in fact represents one half of the infinite environment of the vertical MPS, thus A gives the optimal truncation matrix. All these arguments also apply to V^R and B .

IV. APPLICATIONS

In this section, we apply the TN encoding scheme to 2D classical Ising model and 1D quantum Ising model. There are

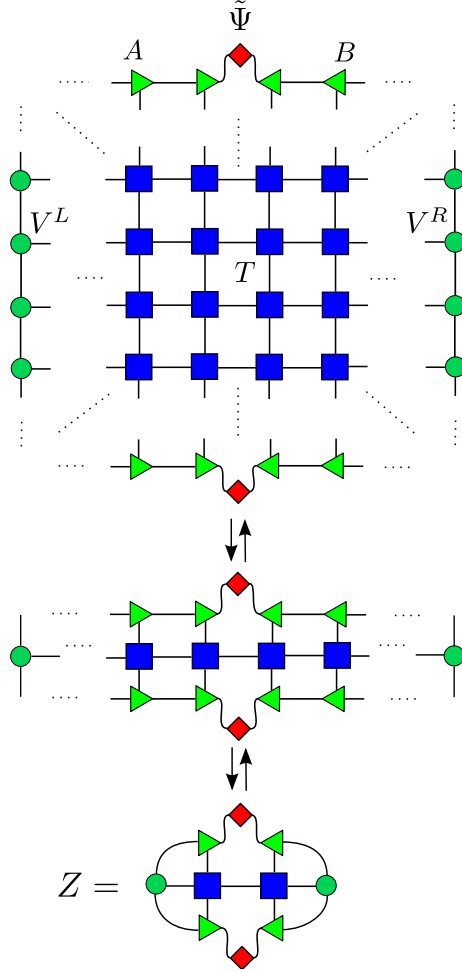


Figure 10. (Color online) The TN encoding given by iDMRG, where the TN contraction is equivalently transformed into a 1D TN and then finally into a local contraction.

intrinsic differences between their TN representations. For the 2D classical partitioning, the two dimensions of the TN are both spatial and discrete, and are equivalent to each other. For the 1D quantum chain, one dimension of the TN is spatial and discrete, and the other is the time dimension that is continuous. Though both models give the same central charge $c = 1/2$ that corresponds to a free fermionic field theory in the real space, we find intrinsically different properties in the imaginary time characterized by the temporal correlations and the corresponding “central charge”. It means that the criticality of a (1 + 1)D theory or a 2D TN should be characterized by two scalings in the two directions of the TN.

A. Two-dimensional classical Ising partition function

To demonstrate the validity of our theory, we study the 2D classical model. Its partition function can be directly written in a 2D TN, where the local tensor is the probability distribution of some local Ising spins. Here, we take the Ising model

on square lattice as an example, where the local tensor is defined as

$$T_{s_1 s_2 s_3 s_4} = e^{-\beta(s_1 s_2 + s_2 s_3 + s_3 s_4 + s_4 s_1)}, \quad (45)$$

with β the inverse temperature and the spin index $s_i = \pm 1$. Note that the local tensor of the TN can also be chosen as the contraction of several T 's.

From the exact solution⁴³, we have the critical temperature $\beta_c = \ln(1 + \sqrt{2})/2$. At the critical temperature, the dominant eigenstate of the transfer matrix can be approximated as an MPS. It is well known that each MPS with a finite bond dimension corresponds to a gapped state with a finite correlation length ξ and entanglement entropy S . the central charge can be extracted by the scaling behavior⁴⁴⁻⁴⁶. Specifically speaking, with different χ , ξ and S satisfy

$$\xi \propto \chi^\kappa, \quad (46)$$

$$S = \frac{c\kappa}{6} \ln \chi + \text{const.} \quad (47)$$

The coefficient gives the central charge $c = 1/2$ that corresponds to a free fermionic field theory⁴⁴. By combining Eqs. (46) and (47), one can readily have

$$S = \frac{c}{6} \ln \xi + \text{const.} \quad (48)$$

which is independent of the calculation parameters.

In Fig. 11, we show that the MPS from iDMRG has the same correlation length ξ and entanglement entropy S as the vertical MPS obtained simultaneous in the iTEBD in the other direction with the difference $O(10^{-5})$. In other words, these two MPS's, though updated within two different schemes and located in two different directions of the TN, are connected by a gauge transformation. By choosing different bond dimension cut-off and cells to construct the tensor T , the relation between ξ and S shows robustly a logarithmic scaling, giving accurately the central charge. The precision increases with the size of the cell tensor.

B. One-dimensional quantum Ising chain

For the ground state of the 1D quantum chain that is essentially a (1+1)D theory, the vertical MPS is defined on the continuous time dimension. Here, we take the 1D quantum Ising chain in a transverse magnetic field as an example, where the Hamiltonian reads

$$H = J \sum_i S_i^x S_{i+1}^x - h \sum_j S_j^z, \quad (49)$$

with S^x and S^z the spin operators on the x and z directions. The ground state has been exactly solved by fermionization⁴⁷ with central charge $c = 0.5$.

The ground state calculation can be transformed to a TN contraction problem⁶ by Trotter-Suzuki decomposition²⁰. The local tensor of the TN is obtained by the imaginary-time evolution operator $e^{-\tau H}$ with the Trotter step τ an infinitesimal real number. Then, we use the approach explained in Sec. III

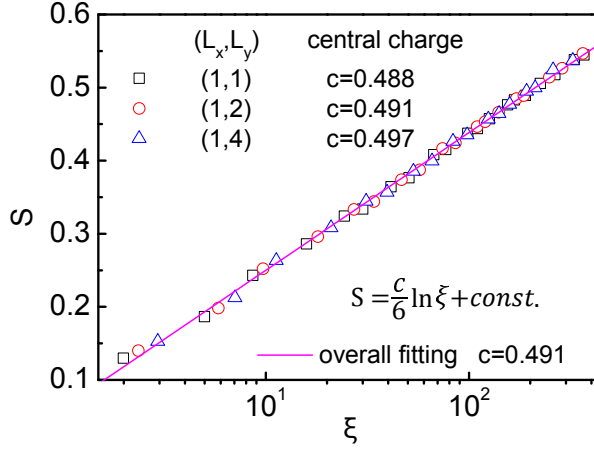


Figure 11. (Color online) The entanglement entropy S against correlation length ξ of the time MPS in 2D Ising model at the critical temperature is given. By varying the dimension cut-off $\chi = 2 \sim 20$ and the cell tensor of size (L_x, L_y) , an intrinsic logarithmic scaling behavior is observed, which is independent of calculation parameters. The central charge c from the fitting with different (L_x, L_y) is accurately obtained (with the exact solution $c = 0.5$). The results from the spatial MPS are the same as those from the time MPS with the difference $\sim O(10^{-5})$.

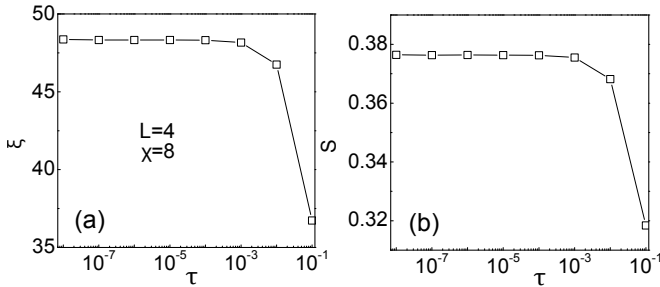


Figure 12. For the spatial MPS that gives the ground state of the Hamiltonian, the correlation length ξ and the entanglement entropy S of the spatial MPS's converge when the Trotter step τ decreases. We take the length of the unit cell $L = 4$ and the bond dimension cut-off $\chi = 8$.

(B) to solve the TN contraction (similar to iDMRG³ but applied directly to TN). The ground state is given by the MPS extended in the spatial direction. In this scheme, another well-defined MPS appears simultaneously in the time direction. It is interesting to see the physical properties of the time MPS as well as its scaling behavior at the critical point.

In Fig. 12, the correlation length ξ and entanglement entropy S of the spatial MPS converges rapidly to finite values as the Trotter step τ decreases. At this situation, the Trotter error that is estimated as $O(\tau^2)$ is negligible.

For the time MPS, its correlation length ξ_T diverges as τ decreases, thus is not well-defined. Considering that the (imaginary) time length is determined by both ξ_T and the Trotter step τ that characterizes the discretization of time, we redefine the time correlation length as $\xi_T \tau$. Fig. 13 (a) shows that $\xi_T \tau$ converges rapidly when reducing τ .

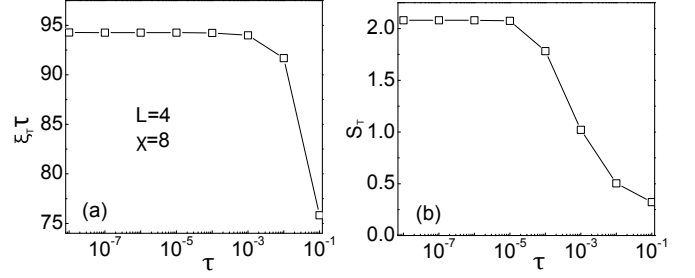


Figure 13. The physical correlation length ξ_{tau} and entanglement entropy S converges when reducing the Trotter step τ . We take the length of the unit cell $L = 4$ and the bond dimension cut-off $\chi = 8$.

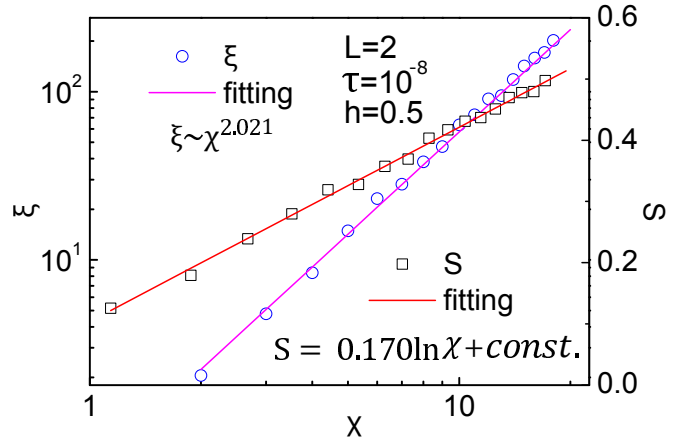


Figure 14. (Color online) The scaling of the correlation length ξ and entanglement entropy S versus the bond dimension cut-off χ of the spatial MPS. We take $h = 0.5$, $L = 2$ and $\tau = 10^{-8}$.

It is known that while using MPS to approximate the ground state at the critical point, its entanglement entropy S fulfills a logarithmic scaling law versus correlation length ξ and the bond dimension χ , as shown in Eqs. (46) and (47)^{44–46}. As shown in Fig. 14, our results with $L = 2$ precisely demonstrate such behaviors.

In Fig. 15, the scaling of S against ξ of the spatial MPS with $L = 2$ and 4 is given. The results accurately give the central charge $c = 0.5$ with an error $O(10^{-3})$. Note that for different choices of L , there are small corrections to both ξ and S versus χ , leading together to better results of c .

The properties of the time MPS are quite different. For the temporal entanglement¹⁸, the time MPS is always maximally entangled, i.e., the entanglement spectrum is flat. It means the temporal entanglement spectrum exactly satisfies the logarithmic scaling law

$$S_T = - \sum \frac{1}{\chi} \ln \frac{1}{\chi} = \ln \chi. \quad (50)$$

The reason is that when the Trotter step τ approaches zero, the evolution of the spatial MPS is nearly identical. Thus as shown in the inset of Fig. 16, the dominant term of the “evolution” of the time MPS is the tensor product with the identity of its “virtual” bonds (which actually are the physical bonds of the spatial MPS). Such temporal entanglement spectrum

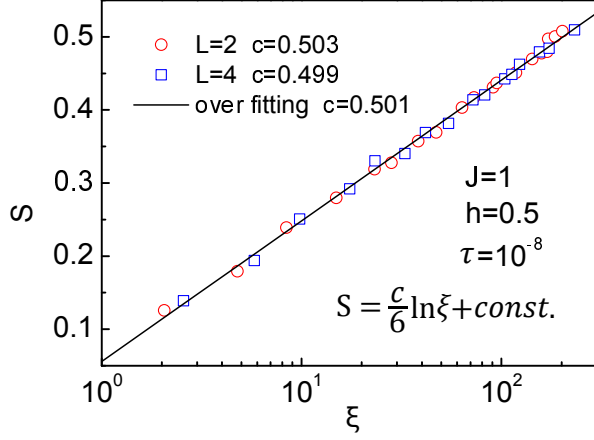


Figure 15. (Color online) By varying the dimension cut-off and the size of the unit cell L , the entanglement entropy S against correlation length ξ of the ground state of 1D transverse Ising chain at the critical magnetic field is given. An intrinsic logarithmic scaling behavior is observed, which is independent of calculation parameters. The central charge c from the fitting with different L is accurately obtained (with the exact solution $c = 0.5$).

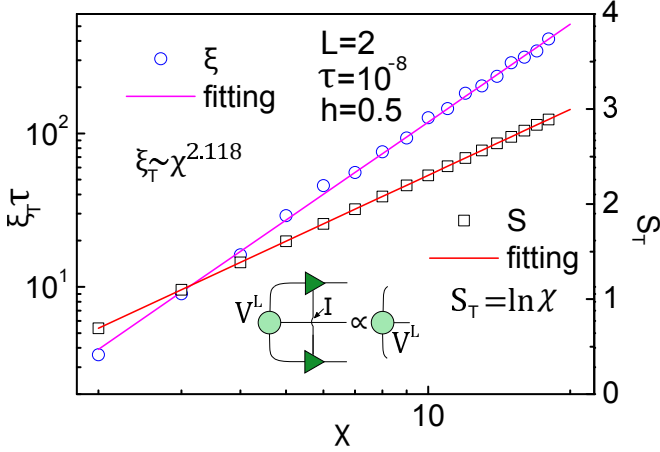


Figure 16. (Color online) The scaling of the correlation length $\xi_T \tau$ and the temporal entanglement entropy S_T versus the bond dimension cut-off χ of the time MPS. We take $h = 0.5$, $L = 2$ and $\tau = 10^{-8}$. The inset shows that when $\tau \rightarrow 0$, the evolution of the time MPS is nearly the tensor product with an identity of its virtual bonds, which makes it maximally entangled.

appears for any magnetic fields, meaning Eq. (50) holds no matter the system is at the critical point or not.

Different from the temporal entanglement, we show that the correlation length ξ_T of the time MPS is actually the dynamic correlation length of the ground state, whose properties rely on the criticality of the model. Taking the transverse Ising chain as an example, the dimensions of time and space have been proven to be equivalent transforming the model into a 2D classical partition function. Two correlation length satisfy

$$\xi \propto \xi_T^z, \quad (51)$$

with the rescaling factor $z = 1$ in this model. Such a relation

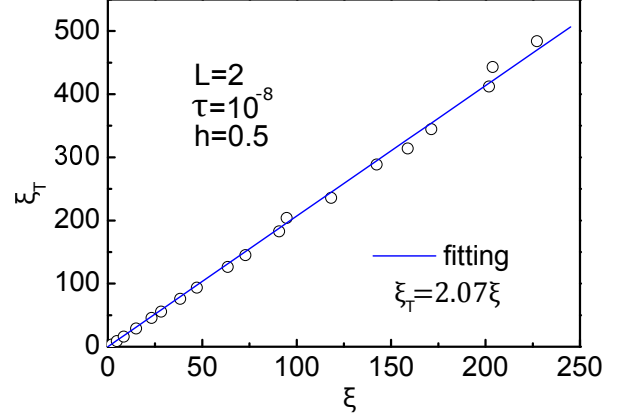


Figure 17. (Color online) The correlation length of the time MPS ξ_T versus that of the spatial MPS ξ . A linear relation is discovered which read $\xi_T = 2.07\xi$, which is consistent with the equivalence between the space and time dimensions of this model.

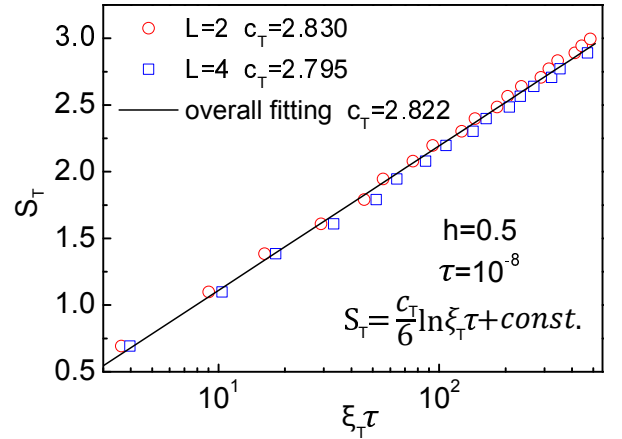


Figure 18. (Color online) By varying the dimension cut-off and the size of the unit cell L , the entanglement entropy S against effective correlation length $\xi_T \tau$ of the time MPS of 1D transverse Ising chain at the critical magnetic field is given. An intrinsic logarithmic scaling behavior is observed, which is independent of calculation parameters. An abnormal central charge c from the fitting with different L is obtained.

is verified at the critical point, as show in Fig. 17.

On the other hand, we find that the time MPS is also critical at $h = 0.5$, satisfying a scaling law against the bond dimension χ that is similar to the spatial MPS. In Fig. 16, we show that ξ_T and S_T satisfy Eqs. (46) with the exponent $\kappa_T \simeq \kappa \simeq 2$ and (50), respectively. By fitting with Eq. (48), one can still define a “temporal central charge” $c_T = 6/\kappa \simeq 2.8$, which is given in Fig. 18 with different χ and L .

For comparison, we show in Fig. 19 $\xi_T \tau$ and S_T of the time MPS at $h = 0.2$ when the magnetic field is away from the critical point. One can see that $\xi_T \tau$ is only $\sim O(1)$ and quickly converges to a finite value as χ increases. On the other hand, S_T still strictly satisfies the logarithmic scaling law given by Eq. (50), meaning the time MPS is maximally entangled just

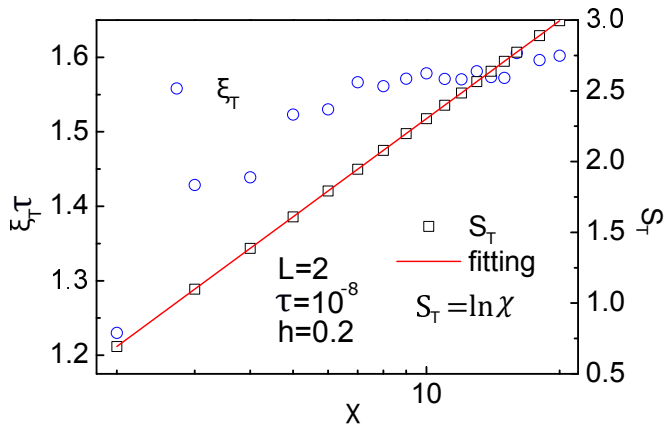


Figure 19. (Color online) At $h = 0.2$, the time MPS is maximally entangled, where the entanglement entropy S_T satisfies the logarithmic scaling law given by Eq. (50). What is different is the correlation length $\xi_T\tau$, which converges to a finite value $O(1)$ rapidly as χ increases.

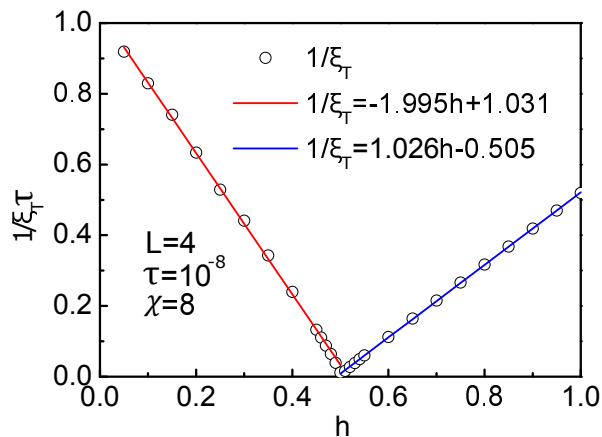


Figure 20. (Color online) The inverse of the correlation length $\xi_T\tau$ of the time MPS is found to bear a linear relation with h . According to Eq. (53), our results suggest that the excitation gap can be accurately obtained from the correlation length of the time MPS.

the same as the critical ground state.

It is known that at a non-critical point, the dynamic corre-

lation function decays exponentially as

$$\langle s_t s_{t+dt} \rangle \propto e^{-\Delta dt}, \quad (52)$$

with Δ the excitation gap. Thus, the excitation gap Δ can be given by the dynamic correlation length as

$$\Delta \propto |h - h_c| \propto \frac{1}{\xi_T\tau}. \quad (53)$$

As shown in Fig. 20, such a relation is precisely found with our scheme, meaning that the excitation gap can be accurately determined from the time MPS.

Our simulations show that the time MPS's at or away from the critical point are both maximally entangled, satisfying the logarithmic scaling given by Eq. (50). Though these two time MPS's have the same entanglement property, it is quite interesting to see that the correlation functions are essentially different. While the entanglement actually gives the properties of the fixed point state (the ground state of the transverse evolution), the correlation length contains the information of the corresponding excitations: the criticality of the evolution determines the scaling behavior of the correlation. But it is still unclear if the scaling coefficient corresponds to a central charge in the conformal field theory.

V. CONCLUSION

In this work, we propose a unified scheme based on the AOP of TN, where the spatial MPS in iDMRG and time MPS in iTEBD are defined in the two directions of the TN. The validity of these two MPS's are shown by applying to the 2D classical Ising model. Then we demonstrate on the 1D transverse Ising model that the time MPS gives the dynamic correlation of the ground state, from which the excitation gap can be accurately obtained. Our scheme can be readily applied to other 1D models, including those defined in continuous space and time. It can also be generalized to simulate the dynamic correlation as well as the excitation gap of 2D quantum systems.

ACKNOWLEDGMENTS

We thank Ian McCulloch for stimulating discussions. This work was supported by ERC ADG OSYRIS, Spanish MINECO (Severo Ochoa grant SEV-2015-0522), FQUS (FIS2013-46768), Catalan AGAUR SGR 874, Fundació Cellex, and EU FETPRO QUIC.

* Corresponding author. Email: shi-ju.ran@icfo.es

¹ S. R. White, *Density matrix formulation for quantum renormalization groups*, Phys. Rev. Lett. **69**, 2863 (1992).

² S. R. White, *Density-matrix algorithms for quantum renormalization groups*, Phys. Rev. B **48**, 10345 (1993).

³ I. P. McCulloch, *Infinite size density matrix renormalization group*, arXiv:0804.2509.

⁴ G. Vidal, *Efficient Classical Simulation of Slightly Entangled Quantum Computations*, Phys. Rev. Lett. **91**, 147902 (2003).

⁵ G. Vidal, *Efficient Simulation of One-Dimensional Quantum Many-Body Systems*, Phys. Rev. Lett. **93**, 040502 (2004).

- ⁶ G. Vidal, *Classical Simulation of Infinite-Size Quantum Lattice Systems in One Spatial Dimension*, Phys. Rev. Lett. **98**, 070201 (2007).
- ⁷ R. Orús and G. Vidal, *Infinite time-evolving block decimation algorithm beyond unitary evolution*, Phys. Rev. B **78**, 155117 (2008).
- ⁸ K. G. Wilson, *The renormalization group: Critical phenomena and the Kondo problem*, Rev. Mod. Phys. **47**, 773 (1975).
- ⁹ R. J. Bursill and T. Xiang and G. A. Gehring, *The density matrix renormalization group for a quantum spin chain at non-zero temperature*, J. Phys. Cond. Matter **8**, L583 (1996).
- ¹⁰ X. Q. Wang and T. Xiang, *Transfer-matrix density-matrix renormalization-group theory for thermodynamics of one-dimensional quantum systems*, Phys. Rev. B **56**, 5061 (1997).
- ¹¹ A. E. Feiguin and S. R. White, *Finite-temperature density matrix renormalization using an enlarged Hilbert space*, Phys. Rev. B **72**, 220401(R) (2005).
- ¹² E. M. Stoudenmire and S. R. White, *Studying Two-Dimensional Systems with the Density Matrix Renormalization Group.*, Ann. Rev. Cond. Matter Phys. **3**, 111 (2012).
- ¹³ G. K.-L. Chan and A. Keselman and N. Nakatani and Z. D. Li and S. R. White, *Matrix Product Operators, Matrix Product States, and ab initio Density Matrix Renormalization Group algorithms*, arXiv: 1605.02611.
- ¹⁴ U. Schollwöck, *The density-matrix renormalization group in the age of matrix product states.*, Ann. Phys. **96**, 326 (2011).
- ¹⁵ I. P. McCulloch, *From density-matrix renormalization group to matrix product states.*, J. Stat. Mech. **2007**, P10014 (2007).
- ¹⁶ E. Tarrico, S.-J. Ran, A. J. Ferris and M. Lewenstein, *An efficient perturbation theory of density matrix renormalization group*, arXiv: 1605.00940.
- ¹⁷ F. Verstraete and J. I. Cirac, *Continuous Matrix Product States for Quantum Fields*, Phys. Rev. Lett. **104**, 190405 (2011).
- ¹⁸ M. B. Hastings and R. Mahajan, *Connecting entanglement in time and space: Improving the folding algorithm*, Phys. Rev. A **91**, 032306 (2015).
- ¹⁹ V. Stojevic, J. Haegeman, I. P. McCulloch, L. Tagliacozzo and F. Verstraete, *Conformal data from finite entanglement scaling*, Phys. Rev. B **91**, 035120 (2015).
- ²⁰ M. Suzuki and M. Inoue, *The ST-Transformation Approach to Analytic Solutions of Quantum Systems. I General Formulations and Basic Limit Theorems*, Prog. Theor. Phys. **78**, 787-799 (1987).
- ²¹ M. Inoue and M. Suzuki, *The ST-Transformation Approach to Analytic Solutions of Quantum Systems. II Transfer-Matrix and Pfaffian Methods*, Prog. Theor. Phys. **79**, 645 (1998).
- ²² M. Levin and C. P. Nave, *Tensor Renormalization Group Approach to Two-Dimensional Classical Lattice Models*, Phys. Rev. Lett. **99**, 120601 (2007).
- ²³ H. C. Jiang, Z. Y. Weng, and T. Xiang, *Accurate Determination of Tensor Network State of Quantum Lattice Models in Two Dimensions*, Phys. Rev. B **101**, 090603 (2008).
- ²⁴ Z. C. Gu, M. Levin, and X. G. Wen, *Tensor-entanglement renormalization group approach as a unified method for symmetry breaking and topological phase transitions*, Phys. Rev. B **78**, 205116 (2008).
- ²⁵ J. Jordan, R. Orús, G. Vidal, F. Verstraete, and J. I. Cirac, *Classical Simulation of Infinite-Size Quantum Lattice Systems in Two Spatial Dimensions*, Phys. Rev. Lett. **101**, 250602 (2008).
- ²⁶ Z. Y. Xie, H. C. Jiang, Q. N. Chen, Z. Y. Weng, and T. Xiang, *Second Renormalization of Tensor-Network States*, Phys. Rev. Lett. **103**, 160601 (2009).
- ²⁷ Z. C. Gu and X. G. Wen, *Tensor-entanglement-filtering renormalization approach and symmetry-protected topological order*, Phys. Rev. B **80**, 155131 (2009).
- ²⁸ R. Orús and G. Vidal, *Simulation of two-dimensional quantum systems on an infinite lattice revisited: Corner transfer matrix for tensor contraction*, Phys. Rev. B **80**, 094403 (2009).
- ²⁹ L. Wang and F. Verstraete, *Cluster update for tensor network states*, arXiv:1110.4362.
- ³⁰ Z. Y. Xie, J. Chen, M. P. Qin, J. W. Zhu, L. P. Yang and T. Xiang, *Coarse-graining renormalization by higher-order singular value decomposition*, Phys. Rev. B **86**, 045139 (2012).
- ³¹ W. Li, J. von Delft and T. Xiang, *Efficient simulation of infinite tree tensor network states on the Bethe lattice*, Phys. Rev. B **86**, 195137 (2012).
- ³² P. Czarnik L. Cincio and J. Dziarmaga, *Projected entangled pair states at finite temperature: Imaginary time evolution with ancillas*, Phys. Rev. B **86**, 245101 (2012).
- ³³ P. Czarnik and J. Dziarmaga, *Projected Entangled Pair States at Finite Temperature: Iterative Self-Consistent Bond Renormalization for Exact Imaginary Time Evolution*, Phys. Rev. B **92**, 035120 (2015).
- ³⁴ H. N. Phien, J. A. Bengua, H. D. Tuan, P. Corboz and R. Orús, *Infinite projected entangled pair states algorithm improved: Fast full update and gauge fixing*, Phys. Rev. B **92**, 035142 (2015).
- ³⁵ S. J. Ran, *Ab initio optimization principle for the ground states of translationally invariant strongly correlated quantum lattice models*, Phys. Rev. E **93**, 053310 (2016).
- ³⁶ A. J. Daley and C. Kollath and U. Schollwöck and G. Vidal, *Time-dependent density-matrix renormalization-group using adaptive effective Hilbert spaces*, J. Stat. Mech.: Theor. Exp., P04005 (2004).
- ³⁷ S. Östlund and S. Rommer, *Thermodynamic Limit of Density Matrix Renormalization*, Phys. Rev. Lett. **75**, 3537 (1995).
- ³⁸ R. Orus, *A Practical Introduction to Tensor Networks: Matrix Product States and Projected Entangled Pair States*, Ann. Phys. **349**, 117 (2014).
- ³⁹ M. Suzuki, *Fractal decomposition of exponential operators with applications to many-body theories and Monte Carlo simulations*, Phys. Lett. A **146**, 319 (1990).
- ⁴⁰ M. Suzuki, *General theory of fractal path integrals with applications to many-body theories and statistical physics*, J. Math. Phys. **32**, 400 (1991).
- ⁴¹ G. M. Crosswhite and A. C. Doherty and G. Vidal, *Applying matrix product operators to model systems with long-range interactions*, Phys. Rev. B **78**, 035116 (2008).
- ⁴² V. Nebendahl and W. Dür, *Improved numerical methods for infinite spin chains with long-range interactions*, Phys. Rev. B **87**, 075413 (2013).
- ⁴³ L. Onsager, *Crystal Statistics. I. A Two-Dimensional Model with an Order-Disorder Transition*, Phys. Rev. **65**, 117 (1944).
- ⁴⁴ G. Vidal, J. I. Latorre, E. Rico and A. Kitaev, *Entanglement in quantum critical phenomena*, Phys. Rev. Lett. **90**, 227902 (2003).
- ⁴⁵ L. Tagliacozzo, T. R. de Oliveira, S. Iblisdir and J. I. Latorre, *Scaling of entanglement support for matrix product states*, Phys. Rev. B **78**, 024410 (2008).
- ⁴⁶ F. Pollmann, S. Mukerjee, A. M. Turner, and J. E. Moore, *Theory of Finite-Entanglement Scaling at One-Dimensional Quantum Critical Points*, Phys. Rev. Lett. **102**, 255701 (2009).
- ⁴⁷ P. Pfeuty, *The one-dimensional Ising model with a transverse field*, Ann. Phys. **57**, 79-90 (1970).